INHIBITION OF Gβγ BUT NOT Gα SIGNALING BY A SMALL MOLECULE PROVIDES EVIDENCE FOR A NEW MECHANISM OF LIGAND BIAS AT A G PROTEIN-COUPLED RECEPTOR

Stefanie Blättermann[1], Lucas Peters[1], Philipp Aaron Ottersbach[2], Andreas Bock[3], Viktoria Konya[4], C. David Weaver[5], Angel Gonzalez[6], Ralf Schröder[1], Rahul Tyagi[7], Petra Luschnig[4], Jürgen Gäb[2], Stephanie Hennen[1], Trond Ulven[7], Leonardo Pardo[6], Klaus Mohr[3], Michael Gütschow[2], Akos Heinemann[4] and Evi Kostenis[1]

[1]Molecular-, Cellular-, and Pharmacobiology Section, Institute of Pharmaceutical Biology, University of Bonn, Nussallee 6, 53115 Bonn, Germany

[2]Pharmaceutical Institute, Pharmaceutical Chemistry I, University of Bonn, An der Immenburg 4, 53121 Bonn, Germany

[3]Pharmacology & Toxicology, University of Bonn, An der Immenburg 4, 53121 Bonn, Germany

[4]Institute of Experimental and Clinical Pharmacology, Medical University of Graz, A-8010 Graz, Austria

[5]1215 MRB IV, Department of Pharmacology, Vanderbilt University, Nashville, TN 37323, USA

[6]Laboratori de Medicina Computacional, Unitat de Bioestadística, Facultat de Medicina, Universitat Autònoma de Barcelona, E-08193 Bellaterra, Barcelona, Spain

[7]Department of Physics and Chemistry, University of Southern Denmark, Campusvej 55, DK-5230 Odense M, Denmark

Corresponding authors: Evi Kostenis

Molecular-, Cellular-, and Pharmacobiology Section

Institute of Pharmaceutical Biology

University of Bonn, 53115 Bonn, Germany

Phone: +49 228 732678/ 733194

Fax: +49 228 733250

Email: kostenis@uni-bonn.de

Akos Heinemann

Institute of Experimental and Clinical Pharmacology

Medical University of Graz, A-8010 Graz, Austria

Phone: +43 316 380 4508

Fax: +43 316 380 9645

Email: akos.heinemann@medunigraz.at

Abstract

Differential targeting of heterotrimeric G protein versus β-arrestin signaling are emerging concepts in G protein-coupled receptor (GPCR) research and drug discovery, and biased engagement by GPCR ligands of either β-arrestin or G protein pathways has been disclosed. Herein we report on the identification of an entirely novel mechanism of ligand bias to titrate signaling specificity of a cell surface GPCR. Using a combination of biomolecular and virtual screening, a small molecule modulator, Gü1654, was identified that is competent to exclusively inhibit Gβγ but not Gα signaling triggered upon activation of $G\alpha_i$-βγ by the chemoattractant receptor OXE-R in both recombinant and human primary cells. Gü1654 does not produce non-specific interference with signaling directly at or downstream of Gβγ. This hitherto unappreciated mechanism of ligand bias at a GPCR highlights both a new paradigm for functional selectivity and a potentially novel strategy to develop pathway-specific therapeutics.

INTRODUCTION

G protein-coupled receptors (GPCRs) are trans-membrane proteins that share a common super-structure consisting of an extracellular N-terminus and an intracellular C-terminus connected by seven α-helical domains[1-5]. Their biological importance has inspired intensive investigations on many fundamental aspects concerning their function and regulation and is reflected by the fact that GPCRs belong to the most commonly targeted protein families for prescribed medicines[6]. GPCRs utilize extracellular and transmembrane regions to sense a variety of physiological stimuli such as neurotransmitters, hormones, chemokines, lipids, and nucleotides among many others. Despite the chemical diversity of the activating ligands, GPCRs do share a common mechanism of relaying information from outside the cell to its interior. Upon binding to extracellular stimuli, GPCRs signal either through heterotrimeric Gα-βγ proteins from different families ($G\alpha_{i/o}$, $G\alpha_{q/11}$, $G\alpha_{s}$, $G\alpha_{12/13}$) and/or – as more recently appreciated – through β-arrestin proteins[5,7-10]. For a large number of GPCRs, engagement of multiple G proteins has been described, in isolation, or in parallel to stimulation of β-arrestin pathways[5,8-14], and a number of ligands have meanwhile been characterized, the pharmacology of which depends on the individual receptor signaling endpoints that are being examined[5,8,10-17]. Ligands that differentially affect downstream pathways are now referred to as biased ligands or functionally selective ligands, and the terms functional selectivity, ligand bias, agonist-trafficking of receptor responses and pluridimensional efficacy have been coined to describe effector-dependent pharmacology of GPCR modulators[5,13,14,18]. Some of the biased agonists have evolved as invaluable tools to deconvolute complex signaling patterns of GPCRs both *in vitro* and *in vivo*[5,9,12]. It could even be envisaged that the concept of ligand bias will translate into novel and more specific approaches for therapeutic intervention and hence become meaningful *in vivo*[8,9]. A characteristic feature of biased ligands is their ability to selectively or preferentially activate one or more effector pathways over others, for example discriminate between individual heterotrimeric G protein pathways or between G

protein and β-arrestin signaling[5,13,14,17-19]. Biased ligands may also display opposing efficacies in a pathway-dependent manner[5,10,13,18,20,21]. Apparently, there is heterogeneity in both the G protein families and β-arrestins that are available for interaction with activated receptors. The numerous examples on biased ligands have resulted in the appreciation that individual ligands may stabilize distinct receptor conformations and that a single receptor may adopt multiple, ligand-specific conformational states[5,10,11,13,14,18,20].

In this study, we present an unprecedented concept for ligand bias, using the receptor for the lipid mediator 5-oxo-6E,8Z,11Z,14Z-eicosatetraenoic acid (5-oxo-ETE), referred to as OXE-R[22-24], as a model system. OXE-R is a $G\alpha_{i/o}$-sensitive receptor that is expressed in eosinophils, neutrophils, basophils and monocytes, and its endogenous agonist 5-oxo-ETE acts as potent chemoattractant for these cells but also as factor regulating survival of tumor cells[22-24]. A large number of downstream signaling events induced by 5-oxo-ETE are mediated via $G\alpha_{i/o}$-βγ heterotrimeric G proteins[22-24], but the pathophysiological role of this ligand receptor pair is not well understood, in part due to the lack of pharmacological tools for this receptor.

Herein, we report on the identification of the first small molecule inhibitor for the OXE-R – Gü1654 – with a hitherto unappreciated mechanism of action: Gü1654 selectively disrupts Gβγ but not $G\alpha_i$ signaling triggered upon activation of the $G\alpha_i$-βγ heterotrimer by OXE-R. Such a βγ-biased mechanism represents an important expansion in the chemical space for GPCR ligands and offers an entirely novel concept of selective interference with the signaling repertoire of cell surface receptors and, therefore, a potentially novel strategy to develop signaling pathway-specific therapeutics.

RESULTS

Receptor-based identification of a novel OXE-R modulator

To identify antagonists for the 5-oxo-ETE receptor OXE-R, for which no small molecule inhibitors are available to date, a biomolecular screening was performed using a subset of our in-house small molecule repository consisting of compounds from natural sources and synthetic ligands in Ca^{2+} mobilization assays on OXE-R-expressing cells. To accomplish this, HEK293 cells, stably transfected to co-express OXE-R and the promiscuous $G\alpha_{16}$ protein, were pre-treated with the potential receptor modulators which were tested for their ability to inhibit intracellular Ca^{2+} flux upon stimulation with the agonist 5-oxo-ETE. The primary screen yielded two structurally closely related ligands (designated as Gü1157 and Gü1158, **Fig. 1a**) that consistently displayed about 30% inhibition of 5-oxo-ETE-mediated Ca^{2+} flux (**Fig. 1b**) but did not trigger Ca^{2+} mobilization on their own (**Fig. 1c**), and thus do not mask inhibition of agonist responses in this assay. For synthetic routes to both inhibitors see **Supplementary Figure 1** and for a detailed description of synthesis and compound characterization see **Supplementary online Methods**. To examine whether the antagonists retain capacity to inhibit OXE-R in its natural environment, chemotactic activation of human eosinophils was chosen as functional assay. Pre-incubation with Gü1157 substantially reduced 5-oxo-ETE-mediated shape change (**Fig. 1d**). No inhibition of shape change by Gü1157 was observed when eosinophils were stimulated with prostaglandin D_2 (**Fig. 1e**) indicating that the antagonistic effect is specific to OXE-R. Unexpectedly, however, neutrophils which also express OXE-R[23,24], were activated in the sole presence of Gü1157, and higher concentrations of this ligand caused non-specific activation of both neutrophils and eosinophils (**Supplementary Figure 2a,b**). In order to identify additional OXE-R antagonists and to minimize biomolecular screening efforts, we chose to perform a virtual screening of the ZINC database (http://zinc.docking.org[25]) using Gü1157 and Gü1158 as baits.

Prior to the virtual screening, the structural requirements for the interaction between the ligands and OXE-R were defined by computational modeling (for details see **Supplementary online Methods**), based on the recently solved x-ray structure of the chemokine receptor CXCR4[2]. Our OXE-R model predicts that a number of charged amino acids ($R150^{2.60}$, $R176^{3.36}$, and $E260^{5.46}$) within the transmembrane (TM) helices point toward the binding site crevice. It seems reasonable to assume that the protonated amine group of Gü1157 and Gü1158 forms an ionic interaction with $E260^{5.46}$ (**Fig. 1f** and **Supplementary Figure 3**). With this anchoring point to the receptor, the central and large aromatic moiety of the ligands expands toward TM 2, to form hydrogen bond interactions between the carbonyl groups and $R176^{3.36}$ and $R150^{2.60}$ and aromatic-aromatic interactions with $F337^{7.35}$. In addition, the terminal phenyl ring of the ligands forms an edge-to-face interaction with $Y153^{2.63}$ and $Y154^{2.64}$ in TM 2 and W158 in the extracellular loop 1 (ECL1).

Based on this computational model, a virtual screen of the ZINC database of commercially available compounds was performed. The best 100 compounds were sorted by the Autodock scoring function and docked into the OXE-R model using the AutoDock Vina virtual screening tools[26]. From these, ten were chosen by visual inspection and acquired from commercial vendors, tested for inhibition of OXE-R-mediated Ca^{2+} release and a single active compound was identified (Zinc code 11852816, hereafter referred to as Gü1654, **Fig. 2a**). Relative to Gü1157 and Gü1158, Gü1654 lacks the protonated amine group but otherwise anchors the OXE-R in a manner similar to the other tested compounds (**Fig. 2b**, compare **Fig. 1f** and **Supplementary Figure 3**). Apparently, the entire molecule including all of its pharmacophoric elements is required for biological activity, since fragmentation of Gü1654 into smaller pieces did not allow identification of fragments or functional groups capable to inhibit OXE-R-mediated Ca^{2+} flux (data not shown). The fragments were designed in an attempt to identify new directions for synthetic optimization but also to generate compounds with improved physicochemical properties, since Gü1654 is rather lipophilic as compared

with Gü1157 and Gü1158, respectively (log $D_{7.4}$ values as a measure for lipophilicity are 5.28 (Gü1654), 1.02 (Gü1157), and 0.87 (Gü1158); for log $D_{7.4}$ determination, see **Supplementary online Methods**).

Chemical synthesis of the OXE-R modulator Gü1654

To further pursue Gü1654 in a number of different cellular assays, it was also prepared by chemical synthesis (**Fig. 2c**, for a detailed description of the synthesis and characterization see **Supplementary online Methods**). After selective *S*-methylation of 6-amino-2-mercaptobenzothiazole **1**, reaction with *in situ* generated acetyl isothiocyanate yielded the acetylthiourea **3**, which was cleaved to the thiourea **4** under basic conditions. Oxidative cyclization of **4** with thionyl chloride[28] facilitated the synthetic entry to the benzo[1,2-*d*:4,3-*d*']bisthiazole scaffold decorated with the two different functional groups. As the two aromatic protons of **5** appeared as two duplets with *ortho* coupling constants in the ^{1}H NMR spectrum, angular (and not linear) annelation of the thiazole rings in **5** could be verified. Acylation of tricycle **5** with diphenylacetyl chloride gave the desired Gü1654.

Gü1654 inhibits various cellular signaling routes of OXE-R in human recombinant and primary cells

Gü1654 was of particular interest since it displayed a number of favorable properties: (i) it inhibits OXE-R-mediated Ca^{2+} mobilization in a concentration-dependent, albeit non-competitive manner (**Fig. 3a,b**) but does not trigger a Ca^{2+} response when applied alone (**Supplementary Figure 4a**); (ii) no inhibition of Ca^{2+} flux was observed when cells were challenged with carbachol to stimulate endogenous $G\alpha_q$-linked muscarinic receptors (**Supplementary Figure 4b**); (iii) efficacious and concentration-dependent inhibition of neutrophil shape change and chemotaxis was observed with no signs of non-specific activation even at high concentrations (**Fig. 3c**,**d**); (iv) likewise, shape change and chemotaxis

of human eosinophils that also express the OXE-R was effectively attenuated (**Fig. 3e**,**f**). Inhibition by Gü1654 of 5-oxo-ETE responses in human leukocytes was specific, since the antagonist was completely ineffective when chemotactic activation of neutrophils and eosinophils was achieved by stimulation with the chemoattractant C5a (**Supplementary Figure 5a**) or prostaglandin D_2 (**Supplementary Figure 5b**), respectively.

Gü1654 does not impair all cellular signaling of OXE-R

In addition to increasing cytosolic calcium ion levels, OXE-R is also known to inhibit forskolin-stimulated cAMP production via coupling to $G\alpha_{i/o}$ proteins, an observation made with CHO cells transfected to stably express this receptor[22]. Inhibition of cAMP formation by 5-oxo-ETE in human primary cells has not been reported to date. We therefore established cAMP inhibition assays in primary human neutrophils and determined whether Gü1654 similarly inhibits 5-oxo-ETE-induced responses via this signaling pathway. Surprisingly, Gü1654 was completely inactive at concentrations sufficient to attenuate neutrophil shape change or chemotaxis, respectively (**Fig. 4a, compare with Fig. 3c,d**). Lack of inhibitory activity of Gü1654 was also assessed using cAMP inhibition assays in HEK293 cells into which OXE-R is added by exogenous expression (**Fig. 4b**). Our data support the notion that this pattern of "selective antagonism" is apparently independent of the cellular background or expression level of OXE-R. In fact, lack of antagonism of Gü1654 is also observed when OXE-R functionality is examined in label-free dynamic mass redistribution (DMR) assays that exclusively monitor $G\alpha_{i/o}$ downstream events triggered by OXE-R (**Fig. 4c**). In contrast, Gü1654 behaves as antagonist, when label-free DMR assays are designed to exclusively capture OXE-R signaling downstream of $G\alpha_{16}$ (**Fig. 4d**,**e**), an observation that is congruent with the results from the initial Ca^{2+} mobilization assays, where $G\alpha_{16}$ co-expression was required to guide OXE-R to the Ca^{2+} mobilization pathway. Importantly, Gü1654 pre-incubation had no impact on $G\alpha_{16}$ activation by the chemoattractant receptor CRTH2

(**Supplementary Figure 6**) indicating that it operates via OXE-R but not via inhibition of signaling at or downstream of $G\alpha_{16}$. Together, Gü1654 therefore apparently represents an antagonist with functional selectivity, incompetent to impair $G\alpha_{i/o}$ downstream signaling of OXE-R.

Gü1654 unveils an unprecedented mechanism of signaling bias at OXE-R

To further corroborate this biased antagonism profile, Gü1654 was examined for its effect on additional neutrophil responses, known to be mediated by engagement of $G\alpha_{i/o}$ proteins. 5-Oxo-ETE is known to induce rapid increases of intracellular Ca^{2+} in human neutrophils in a PTX-sensitive manner[24,28] implicating $G\alpha_i$-$\beta\gamma$ proteins in the signaling process. We do confirm PTX-sensitivity of 5-oxo-ETE-mediated Ca^{2+} flux in human neutrophils (**Fig. 5a**); strikingly, however, Gü1654 pre-treatment completely abolished this $G\alpha_{i/o}$-dependent response (**Fig. 5b**). For control, Gü1654 had no effect on interleukin-8 (IL-8)-dependent increases of Ca^{2+} in neutrophils confirming that the antagonistic effect is specific to OXE-R (**Supplementary Figure 7**). Essentially identical results were obtained when human eosinophils were exposed to 5-oxo-ETE and intracellular Ca^{2+} was recorded (**Fig. 5c**,**d**). These cells are also known to transmit their Ca^{2+} signals in a $G\alpha_{i/o}$-sensitive manner[24]. Many chemoattractant activators of leukocytes signal via $G\alpha_{i/o}$-linked GPCRs and their Ca^{2+} signaling can be specifically obliterated in the presence of pertussis toxin, which inactivates heterotrimeric $G\alpha_{i/o}$-$\beta\gamma$ proteins[29]. However, it has become apparent that PTX-sensitive chemoattractant responses such as Ca^{2+} mobilization or even chemotaxis in leukocytes are not transduced by $G\alpha_{i/o}$ subunits but instead triggered by the $G\beta\gamma$ complexes released upon $G\alpha_i$-$\beta\gamma$ heterotrimer activation[29-31]. Indeed, the $G\alpha_i$-$\beta\gamma$-PLCβ2/3 module was found to be responsible for chemoattractant-induced PLC activation and Ca^{2+} mobilization[32] since mice lacking both PLCβ2 and PLCβ3 were unresponsive to chemoattractants in PLC and Ca^{2+} flux

assays[33]. In line with this postulated mechanism, inhibition of Ca^{2+} flux in eosinophils and neutrophils was sensitive to pre-treatment with the PLC inhibitor U73122 but not its inactive analog (**Fig. 5e**,**f**). Hence, the apparent paradoxon, i.e. inhibition by Gü1654 of PTX-sensitive Ca^{2+} flux but lack of antagonistic efficacy in cAMP assays can only be rationalized if Gü1654 was competent to differentially modulate $G\alpha_{i/o}$ versus $G\beta\gamma$-triggered signaling events, a mode of biased antagonism which is unprecedented in the literature so far.

Gü1654 exclusively inhibits $G\beta\gamma$ but not $G\alpha_i$ signaling triggered upon OXE-R activation

To further ascertain that Gü1654 permits $G\alpha_{i/o}$ but not $G\beta\gamma$ signaling of OXE-R, two functional assays were established to exclusively monitor $G\beta\gamma$-dependent downstream events. First, HEK293 cells were transiently transfected to co-express OXE-R, $G\beta_1$ and $G\gamma_2$, respectively, and $G\beta\gamma$-mediated inositol phosphate (IP) production was quantified as a measure of receptor activity. 5-Oxo-ETE-mediated IP production was highly significant and mediated by $G\beta\gamma$, since pre-treatment with the small molecule $G\beta\gamma$ inhibitor gallein[34] completely abolished the response (**Fig. 6a**). Gallein, conversely, hardly affected IP accumulation induced upon stimulation of endogenous $G\alpha_q$-linked muscarinic receptors in agreement with the inability of small molecule $G\beta\gamma$ inhibitors to dampen $G\alpha_q$-mediated cellular responses[34]. Importantly, Gü1654 – ineffective when applied alone – completely abrogated OXE-R-mediated IP production but had no impact on IP levels triggered by stimulation of endogenous $G\alpha_q$-linked muscarinic receptors (**Fig. 6a**) confirming that inhibition of IP production is specific to the OXE-R receptor. In addition, Gü1654 did not impact $G\beta\gamma$-mediated IP accumulation induced upon stimulation of the $G\alpha_i$-linked muscarinic M2 receptor further corroborating that it acts through OXE-R but does not dampen $G\beta\gamma$ downstream signalling in general (**Supplementary Figure 8**).

Exclusive inhibition by Gü1654 of Gβγ signalling was also observed when OXE-R activity was captured with an assay that records Gβγ-mediated opening of G-protein regulated inwardly rectifying K^+ channel (GIRK). It is well established that Gβγ subunits, "released" upon activation of $G\alpha_{i/o}$-coupled receptors, directly interact with GIRK channels and thereby modulate channel opening[35] (for review see[36]). Since GIRK channels also conduct thallium ions, this property has recently been exploited in thallium flux assays as novel platform to monitor Gβγ-mediated signaling triggered by $G\alpha_{i/o}$-sensitive GPCRs[37]. As expected, treatment of HEK-GIRK cells transfected to co-express the OXE-R and pre-loaded with the fluorescent indicator dye BTC-AM responded with robust and concentration-dependent increases in thallium conductance (**Fig. 6b**,**c**). No alterations of thallium conductance upon application of 5-oxo-ETE were observed in HEK-GIRK cells lacking the OXE-R (**Supplementary Figure 9**). In agreement with the postulated mechanism for GIRK channel activation, 5-oxo-ETE responses were completely blunted in cells pre-treated over night with PTX (**Fig. 6c**) or in cells pre-treated for 30 min with the OXE-R antagonist Gü1654 (**Fig. 6d**). Importantly, Gü1654 was ineffective, when Gβγ-mediated opening of GIRK channels was triggered with serotonin via the $G\alpha_{i/o}$-sensitive 5-HT1a receptor (**Supplementary Figure 10**) again corroborating the notion that Gü1654 interdicts Gβγ signaling of the OXE-R but does not blunt function of Gβγ-mediated effectors in general.

Gü1654 spatially separates OXE-R from the Gβγ complex

To the best of our knowledge, all functionally selective ligands reported so far for GPCRs can discriminate between subfamilies of distinct Gα-βγ heterotrimers or between G protein and β-arrestin signaling[5,8-14,17,19,21]. However, differentiation between Gα and Gβγ signaling of distinct heterotrimers in a receptor-dependent manner has not been achieved to date. To gain mechanistic insight into this novel mode of biased antagonism, we assessed whether Gü1654

affects proximity between or relative orientation of the receptor and the Gβγ complex, using a protein-protein-interaction-based bioluminescence resonance energy transfer (BRET) assay. Since previous studies suggested that BRET between receptor and Gβγ is an indicator of conformational changes propagated from an activated receptor to the G protein[38], and since a computational OXE-R-Gα-βγ model based on the crystal structure of the β_2-adrenergic receptor in complex with the Gs heterotrimer (PDB code 3SN6)[39] suggest that the OXE-R-C-terminus expands intracellularly towards the N-termini of Gβ and Gγ (**Supplementary Figure 11**), we reasoned that such assay should prove useful to unravel whether Gü1654 may prevent the 5-oxo-ETE-bound receptor from achieving a conformation required to relay receptor activity to G protein activation. To this end, OXE-R was tagged at its C-terminus with the energy donor Renilla luciferase (RLuc) while $G\beta_1$ and $G\gamma_2$ subunits were N-terminally fused to the energy acceptor GFP10[38,40]. Addition of RLuc to the receptor's C-terminus did not alter its functionality as determined in label-free DMR assays (**Supplementary Figure 12**) and functionality of the Gβ and Gγ BRET probes was described previously[40]. Upon stimulation with 5-oxo-ETE, robust engagement of Gβγ was observed, indicating either de novo association between OXE-R and Gβγ or a conformational change between a preformed OXE-R-Gβγ complex in which energy donor and energy acceptor move closer together (**Fig. 7a**,**b**).

Interestingly, the 5-oxo-ETE-induced BRET response between receptor and Gγ was reduced by 40% in the presence of Gü1654 (**Fig. 7a**), while receptor-Gβ BRET was hardly affected (**Fig. 7b**). These data suggest that Gü1654 prevents – at least in part - communication between the ligand-activated OXE-R and the Gβγ complex by altering their proximity or relative orientation, respectively. Such molecular rearrangement is conceivable given the flexibility of the N-terminal α-helices of Gβ and Gγ, together with the spatial flexibility of the receptor's

C-tail (**Supplementary Figure 13**). Gü1654 – when applied alone - did not affect basal OXE-R-Gβγ BRET (**Fig. 7c**,**d**) reflecting inability to separate a preformed receptor-Gβγ complex. Importantly, when BRET was accomplished between the nicotinic acid receptor HM74A fused to RLuc and the respective Gβγ probe (GFP10-$G\gamma_2$), no inhibition of protein-protein interaction was achieved by Gü1654 (**Fig. 7e**), suggesting that interaction between OXE-R and the Gγ component of the Gβγ complex is specifically inhibited by Gü1654. Finally, Gü1654 was completely ineffective when tested for its ability to inhibit opening of the $G\alpha_i$ nucleotide binding pocket (**Fig. 7f**) as determined in BRET assays with appropriate sensors for the $G\alpha_i$ subunit and the Gβγ complex ($G\alpha_{i1}$-91-RLuc, GFP10-$G\gamma_2$)[38,40]. Lack of antagonism in this assay is well in agreement with the absence of antagonist efficacy in $G\alpha_{i/o}$-based signaling assays. Together, these results provide further support for the hypothesis that Gü1654 interferes with agonist-induced receptor signaling in a manner to permit $G\alpha_i$ but preclude Gβγ activity within an individual Gα-βγ heterotrimer.

DISCUSSION

G protein-coupled receptors (GPCRs) communicate with cells by disassembling or rearranging G protein Gα-βγ heterotrimers into Gα and Gβγ complexes which in turn affect numerous intracellular effectors[5,38,41]. GPCRs may also signal cells by β-arrestin proteins, which have different effector pathways than G proteins[5,8,9,12]. Ligand bias is an emerging concept in GPCR basic research and drug discovery, and a number of functionally selective ligands for GPCRs have been described that either discriminate between distinct Gα-βγ heterotrimers[5,11,19] or differentially affect heterotrimeric G protein versus β-arrestin signaling[5,8-10,17,20]. To the best of our knowledge, we show here - for the first time - that functionally selective ligands may also discriminate between Gα- and Gβγ-mediated downstream events. A small molecule antagonist, Gü1654, was identified that exhibits no significant inhibition of $G\alpha_i$-dependent signaling of the chemoattractant receptor OXE-R in both recombinant and human primary cells, but completely prevented signaling via the Gβγ route as evidenced in Ca^{2+} assays on primary human leukocytes and also in inositol phosphate and thallium flux assays in human recombinant cells engineered to over-express OXE-R. The latter two recombinant assays rely completely on transduction of signals from receptors by the G protein βγ subunits.

This entirely unappreciated mode of ligand bias offers a new perspective to fine-tune GPCR signaling and suggests that modulation of receptor function by pharmacological tools and ultimately medical therapeutics may even be much more flexible and specific than previously anticipated. This is particularly so, if the remaining Gα-βγ subfamilies ($G\alpha_s$, $G\alpha_{q/11}$, $G\alpha_{12/13}$) were equally susceptible to this differential mode of inhibition.

Differentiating between Gα and Gβγ effects is not unprecedented in the literature. In fact, it has already been appreciated over two decades ago that the muscarinic acetylcholine receptor

M2 inhibits adenylyl cyclase and stimulates IP accumulation[42] and that both processes were mediated via $G\alpha_{i/o}$ proteins, as evidenced by their sensitivity to PTX pre-treatment. Intriguingly, however, the adenylyl cyclase response was about 10-fold more sensitive to PTX as compared with the IP response. The authors suggested that both effects are differentially coupled via the same G protein. Indeed, inhibition of adenylyl cyclase is mediated via $G\alpha_{i/o}$ subunits whereas phosphoinositide hydrolysis is mediated by the $G\beta\gamma$ complex "released" upon $G\alpha_i$-$\beta\gamma$ activation[43,44]. These data therefore provide additional support for the notion that differential modulation of $G\alpha$ versus $G\beta\gamma$ responses is indeed achievable.

Conformation-specific allosteric antagonism of GPCRs has previously been disclosed as an interesting concept to direct receptors to certain signaling pathways while simultaneously dispelling them from others[21]. A compound, designated LPI805, inhibits the cAMP response induced by neurokinin A via the NK2 receptor but slightly enhances the agonist's ability to mobilize Ca^{2+} from intracellular stores via the $G\alpha_q$ pathway. Although LPI805 represented the first conformation-specific allosteric antagonist of a GPCR, these data were reminiscent of a number of studies in which ligands were described that display either positive or negative efficacy when assessed in different functional assays[5,8,10,18]. Notably, all of these "protean" ligands regulate separate cellular signals via different G protein heterotrimers or in a G protein-independent manner, but the observation that ligand efficacy may vary in a G protein subunit ($G\alpha$ vs $G\beta\gamma$)-specific manner as described herein is entirely novel.

It is widely accepted that different ligands stabilize distinct conformational states of receptors [5,8,11,12,14]. Apparently, Gü1654 selectively stabilizes a receptor conformation that preserves activation by 5-oxo-ETE of $G\alpha_i$-mediated downstream events such as inhibition of forskolin-activated adenylyl cyclase, but completely precludes propagation of the $G\beta\gamma$-mediated signal.

Models of receptor-G protein interaction presume that $G\beta\gamma$ subunits either play a passive role for nucleotide exchange on $G\alpha$, *i.e.* contribute by scaffolding $G\alpha$ at the plasma membrane via

the prenylated C-terminus of Gγ, or, alternatively, participate actively as suggested by the gear shift and the lever-arm hypothesis[7,31,45]. Although the exact mechanism by which GPCRs trigger Gα nucleotide exchange remains to be fully elucidated, all of these models imply, that decreasing the proximity between an activated receptor and the Gβγ dimer should lead to impaired G protein activation.

Indeed, BRET experiments monitoring proximity between an OXE-R-RLuc fusion protein and the Gβγ complex revealed that robust recruitment by OXE-R of Gγ was reduced by about 40% in the presence of Gü1654 while proximity between OXE-R and Gβ was hardly affected in the Gü1654-occupied receptor (**Fig. 7a**,**b**). Intriguingly, this partial reduction of receptor-Gγ BRET was sufficient to completely silence Gβγ- but not Gα-dependent downstream signaling of OXE-R (**Fig. 6a**, compare with **Fig. 4a-c**). It is tempting to speculate that this partial BRET inhibition is the basis for Gβγ-biased antagonism whereas complete inhibition of OXE-R-Gβγ BRET may be associated with silencing of the entire Gα-βγ heterotrimer signaling repertoire. Indeed, the inverse agonist ICI118551 for the β_2 adrenergic receptor (β_2AR) that completely blocked isoproterenol-induced energy transfer between receptor and Gβγ, also abrogated $G\alpha_s$ activity of the receptor[40]. Similarly, when protein-protein interaction between the α2A adrenoceptor and Gβγ was prevented by the α2A receptor antagonist RX821002, $G\alpha_i$ activation of the receptor was completely blunted[38]. Gü1654, in contrast, does not hinder $G\alpha_i$-GTP from activating its downstream effectors (**Fig. 4a-c**), nor does it interfere with opening of the $G\alpha_i$-nucleotide binding pocket as determined with a BRET sensor pair that is sensitive to detect the structural rearrangements that occur during nucleotide exchange (**Fig. 7f**)[38,40]. Inhibition of Gβγ but not Gα signaling by a given GPCR is surprising because it is typically assumed that once the heterotrimeric G-protein is activated by agonist binding to the GPCR, that subsequent effects of Gβγ and Gα proceed independently of the receptor. Inhibition of Gβγ but not Gα signaling is therefore difficult to

reconcile with the model that G protein α and βγ subunits dissociate upon receptor activation. Our data rather support the notion that G protein α and βγ likely undergo an intramolecular rearrangement during the receptor-mediated GDP-GTP on-off cycle[38,41]. In this complex between receptor, Gα and Gβγ, Gü1654 acts to keep Gβγ apart from the receptor, sufficient to preclude Gβγ-effector activation, yet insufficient to impair nucleotide exchange on Gα. A schematic representation of this novel mode of Gβγ-biased antagonism of GPCRs is presented in **Fig. 8**.

Since Gβγ subunits do not undergo conformational changes after Gα activation, and since Gα nucleotide exchange is achievable in the presence of Gü1654 (**Fig. 4a** and **7f**), our data suggest that Gβγ does not utilize the signaling surface that is exposed on Gβγ after Gα activation for interaction with its downstream target PLCβ. As both PLCβ substrates (phosphatidyl-inositol-4.5-bisphosphate) and stimulators (such as Gβγ) are located at the inner leaflet of the cytoplasmic membrane, it is tempting to speculate that spatial disruption of the interface between Gβγ and the receptor within a multimeric receptor-Gα-βγ-PLC signalling complex is a novel means to selectively silence Gβγ downstream signaling by small molecule modulators targeting cell surface GPCRs.

Such a permissive form of antagonism can only be explained by an allosteric phenomenon since Gü1654 causes the natural agonist 5-oxo-ETE to change its signaling pattern from activation of Gα and Gβγ responses to exclusive Gα activation which can only be rationalized by simultaneous co-occupation of OXE-R with both ligands. Interestingly, OXE-R occupation by Gü1654 shares common structural features as compared with the chemokine receptor CXCR4 bound to a small molecule antagonist IT1t[2]: IT1t binds to CXCR4 in a cavity between TMs 2, 3, and 7 (**Supplementary Figure 14a**). In addition, 1-Oleoyl-R-glycerol (OLC) inserts into the TM bundle from the lipid bilayer via the interface between TMs 5 and 6[2]. The remarkable structural similarity between OLC and 5-oxo-ETE led us to propose - as a

working hypothesis – similar simultaneous binding poses for IT1t and OLC to CXCR4, and Gü1654 and 5-oxo-ETE to OXE-R, respectively (**Supplementary Figure 14b**, compare **Fig. 2b**). The insurmountable nature of antagonism observed with Gü1654 in the various functional assays is in good agreement with such an allosteric mode of action. It will be interesting to determine the consequences of biased antagonism *in vivo* since therapeutic situations that may benefit from biased agonists may in principle also qualify for intervention with biased antagonists.

In spite of its inability to suppress $G\alpha_i$-mediated downstream signaling in human recombinant and primary hematopoietic cells (**Fig. 4a-c**), Gü1654 does represent a suitable pharmacological tool to explore 5-oxo-ETE-mediated signaling and OXE-R physiology *ex vivo* in cells where the receptor is expressed in its natural environment: Gü1654 suppresses a number of leukocyte functions such as Ca^{2+} mobilization, shape change and chemotaxis of both human eosinophils and neutrophils, which implies that all of these responses are unlikely mediated by $G\alpha_{i/o}$ proteins. This is an intriguing finding because GPCRs are classified according to the nature of the $G\alpha$ subunit they specifically recognize although the role of $G\alpha$ itself as signal transducer may be rather minor, at least with respect to transmitting chemotactic responses of OXE-R in human leukocytes.

In this context a novel class of small molecules is noteworthy, specifically designed to inhibit signaling of $G\beta\gamma$ responses without affecting functionality of $G\alpha$ proteins[31,34]. These mechanistically interesting $G\beta\gamma$-inhibitors are thought to improve therapeutic options for a number of diseases in which $G\beta\gamma$ subunits represent central participants[31]. Inhibition of $G\beta\gamma$ by small molecule interaction with the "hotspot" on this protein complex interferes with downstream signaling in a receptor-independent but partially effector-selective way[31,34]. Gü1654, on the contrary, offers the perspective to suppress $G\beta\gamma$ signaling in a strictly receptor-dependent manner. Notably, many drug screening assays are designed to detect

signaling downstream of Gα proteins such as increase of intracellular Ca^{2+} or inositol phosphates for $G\alpha_q$-linked receptors, increase or decrease of cAMP for $G\alpha_s$ and $G\alpha_i$-coupled receptors, respectively, or are based on detection of β–arrestin recruitment[5,8,9,12]. Such assays may not be equally suitable to detect signaling via the Gβγ pathway. Screening of a compound library for OXE-R antagonists using a classical endpoint assay on the natural $G\alpha_{i/o}$ signaling pathway of this receptor would not have permitted identification of Gü1654. The findings of this study are therefore highly relevant for design of appropriate assays in drug discovery and development.

In conclusion, we report identification and characterization of the first GPCR antagonist with striking disparity of efficacy for $G\alpha_i$ versus Gβγ-mediated cellular events. Discrimination of receptor signaling on the level of an individual Gα-βγ heterotrimer has not been achieved to date and suggests an ever increasing number of relevant conformational states that may be adopted by GPCRs and be linked to defined signaling routes. In general, our study opens new vistas for GPCR signaling with significant implication for design of new classes of therapeutics to achieve an unprecedented level of fine-tuning of receptor responses *in vivo* as well as increases the scope for therapeutically targeted selective drug effects.

METHODS

Materials and reagents. See **Supplementary online Methods**.

Complementary DNA (cDNA) expression vectors. See **Supplementary online Methods**.

Cell culture and transfection

Human embryonic kidney (HEK293) cells were maintained in Dulbecco´s modified Eagle´s medium (DMEM) supplemented with 10 % (v/v) FCS, 100 U/ml penicillin, and 100 µg/ml streptomycin at 37°C in a humidified 5% CO_2 atmosphere. Flp-In^{TM}-Chinese hamster ovary cells (Flp-In^{TM}-CHO) stably expressing the M2 receptor (M2-CHO cells) were cultured in Ham's nutrient mixture F-12 (HAM-F12) supplemented with 10% (v/v) FCS, 100 U/ml penicillin, 100 µg/ml streptomycin, and 2 mM L-glutamine. HEK293 cells were transiently transfected 24 h after seeding using the Ca^{2+} phosphate co-precipitation method[46], except for the BRET studies, where electroporation was used for efficient DNA transfer. See **Supplementary online Methods** for details on HEK293 electroporation. For inositol phosphate (IP1) assays, cells were transfected using a total amount of 20 µg cDNA (3 µg OXE-R, 6 µg β_1 and 3 µg γ_2, 8 µg pcDNA3.1).

Generation of stable HEK-OXE-R-Gα_{16} cells

HEK293 cells were transfected to co-express the OXE receptor OXE-R[23] and the promiscuous Gα_{16} protein. Stable clones were maintained in Dulbecco´s modified Eagle´s medium (DMEM) supplemented with 10 % (v/v) FCS, 100 U/ml penicillin, 100 µg/ml streptomycin, and the selection agents hygromycin B (250 µg/ml) and geneticin (400 µg/ml).

Ca^{2+} mobilization assays in HEK293-OXE-R-Gα_{16} cells

HEK293-OXE-R-Gα_{16} cells were seeded at a density of 60,000 cells/well into poly-D-lysine-coated 96-well tissue culture plates, and intracellular Ca^{2+} levels were quantified 24 h later using the Calcium4 assay kit (Molecular devices, CA, USA) as described previously[47].

cAMP accumulation assay in recombinant cells

Levels of intracellular cAMP were quantified as described previously in detail[48] with the HTRF®-cAMP dynamic kit (Cisbio, Bagnols-sur-Cèze Cedex, France) on a Mithras LB 940 reader (Berthold Technologies, Bad Wildbad, Germany) following the manufacturer's instructions.

cAMP accumulation assay in human primary cells

Levels of intracellular cAMP in human neutrophils were quantified with the time-resolved fluorescence resonance energy transfer (TR-FRET) immunoassay kit LANCE® Ultra (Perkin Elmer) as per manufacturer's instructions on the Mithras LB 940 reader.

Inositol phosphate (IP) accumulation assay

Levels of intracellular inositol phosphate (IP1) in HEK293 cells transfected to transiently express the OXE-R along with Gβ_1 and Gγ_2 or in M2-CHO cells (100,000 cells/well each) were quantified as described previously[49] using the HTRF®-IP1 kit (Cisbio, Bagnols-sur-Cèze Cedex, France) as per manufacturer's instructions. For quantification of IP1 levels in the absence of Gα_i activity, cells were pre-treated for 18-24 h with 100 ng/ml PTX. Viability of PTX-treated cells was verified with 300 µM of the pan G protein agonist $AlF4^-$.

Thallium conductance assays

Thallium conductance in HEK-GIRK cells transiently transfected to co-express the OXE-R was recorded as described previously[37]. For details on transfection of HEK-GIRK cells, cell culture, cell plating, dye loading, kinetic imaging and data analysis see **Supplementary online Methods**.

Dynamic mass redistribution (DMR) assays (Corning® Epic® Biosensor measurements)

DMR assays were performed on a beta version of the Corning® Epic® biosensor as described previously in detail[46]. Briefly, HEK293-OXE-R-Gα_{16} cells or HEK293 cells transfected to transiently express OXE-R or a OXE-R-Rluc fusion protein were grown to confluence for 20–24 h on fibronectin-coated Epic® biosensor 384-well microplates. Cells were then washed twice with HBSS containing 20 mM HEPES and kept for at least 1 h in the Epic® reader at 28 °C. DMR was monitored before (baseline read) and after the addition of compound solutions for 2,400 s. A detailed description of the optical biosensor assay is available in **Supplementary online Methods**.

Bioluminescence Resonance Energy Transfer (BRET) assay

All BRET measurements were performed using HEK293 cells transiently co-transfected by electroporation with the indicated BRET partners. BRET constructs and the cDNA amounts used in the individual BRET experiments are described in detail in the **Supplementary online Methods** section.

Molecular modeling and virtual screening

Generation of the OXE-R model, ligand docking and virtual screening of the commercially available ZINC database (http://zinc.docking.org) are described in detail in the **Supplementary online Methods** section.

Preparation of human leukocytes

Citrated whole blood was obtained from healthy non-atopic volunteers after informed consent in agreement with the Institutional Review Board. Polymorphonuclear leukocytes (PMNL, containing neutrophils and eosinophils) were prepared by dextran sedimentation of erythrocytes and Histopaque gradient centrifugation[50]. Purified eosinophil preparations were obtained by negative magnetic selection using antibody cocktails (CD2, CD14, CD16, CD19, CD56, and glycophorin A) and colloidal magnetic particles from StemCell Technologies (Vancouver, Canada).

Chemotaxis

Purified eosinophils were resuspended in assay buffer at 2 x 10^6 cells/ml and 50 µl of the cell-suspension were loaded into the top wells of 48-well microBoyden chemotaxis chamber. 30 µl of assay buffer or agonists were placed into the bottom wells of the chamber, separated from the bottom wells by a 5 µm pore-size polyvinylpyrrolidone-free polycarbonate filter. The chamber was incubated at 37°C for 1 h in a humidified incubator. Migrated cells were enumerated by flow cytometry.

Leukocyte shape change assay

Aliquots of PMNL were mixed with agonists at a final volume of 100 µl and stimulated for 4 min at 37°C. 250 µl of ice-cold fixative solution was added and changes in the cell shape were

estimated as the increase of forward scatter by flow cytometry. Eosinophils were distinguished from neutrophils by autofluorescence in FL-1 and FL-2.

Calcium ion (Ca^{2+}) flux in eosinophils and neutrophils

Intracellular Ca^{2+} levels in eosinophils were analyzed by flow cytometry. PMNL were treated with 2 µM of the acetoxymethyl ester of FLUO-3 in the presence of 0.02% pluronic F-127 for 60 minutes at RT. Changes in intracellular Ca^{2+} levels were detected by flow cytometry as the increase of the fluorescence of the Ca^{2+} sensitive dye FLUO-3 in the FL1-channel. Eosinophils were identified as CD16-negative cells, neutrophils as CD16-positive cells.

Calculations and Data Analysis:

Quantification of DMR signals for concentration-effect curves was performed by calculation of the maximum value between 500 and 1,800 s. All optical DMR recordings were buffer-corrected. For data normalization, indicated as relative response (%), top levels of concentration-effect curves were set 100 % and bottom levels 0 %. Data calculation and EC_{50} value determination by nonlinear regression was performed using Prism 4.02 (Graph Pad, San Diego, CA, USA).

Statistical analyses

Data are shown as mean ± or + S.E. for *n* observations. Comparisons of groups were performed using one-way ANOVA with Bonferroni's multiple comparison test.

ACKNOWLEDGEMENTS

We thank Ulrike Rick and Marianne Vasmer-Ehses for excellent technical assistance and Corning® Inc. for their support on the Epic® system. This work was funded by grants from the Austrian Science Funds FWF (P-22521 to AH), a L'Oreal Fellowship to PL., and a fellowship of the German Research Foundation (Graduate College 804) to P.A.O..

AUTHOR CONTRIBUTIONS

S.B. designed and performed experiments and provided important ideas. L.P[1]., P.A.O., A.B., V.K., C.D.W., R.S., P.L., J.G., and S.H. designed and performed experiments. A.G. and L.P[6]. created the receptor model, performed the virtual screening, and contributed to discussion. R.T. and T.U. established synthesis of 5-oxo-ETE, edited the manuscript and contributed to discussion. C.D.W., L.P[6], K.M., M.G., and A.H. designed research, contributed to discussion, and edited the manuscript. E.K. designed research and wrote the manuscript.

DISCLOSURES

The authors have no financial conflict of interest.

References

1. Rosenbaum, D. M. Rasmussen, S. G. F. & Kobilka, B. K. The structure and function of G-protein-coupled receptors, *Nature* **459,** 356–363 (2009).
2. Wu, B. *et al.* Structures of the CXCR4 Chemokine GPCR with Small-Molecule and Cyclic Peptide Antagonists, *Science* **330,** 1066–1071 (2010).
3. Rasmussen, S. G. F. *et al.* Structure of a nanobody-stabilized active state of the β2 adrenoceptor, *Nature* **469,** 175–180 (2011).
4. Warne, T. *et al.* The structural basis for agonist and partial agonist action on a β1-adrenergic receptor, *Nature* **469,** 241–244 (2011).
5. Kenakin, T. & Miller, L. J. Seven Transmembrane Receptors as Shapeshifting Proteins: The Impact of Allosteric Modulation and Functional Selectivity on New Drug Discovery, *Pharmacological Reviews* **62,** 265–304 (2010).
6. Overington, J. P. Al-Lazikani, B. & Hopkins, A. L. How many drug targets are there?, *Nat. Rev. Drug Discov.* **5,** 993–996 (2006).
7. Bourne, H. R. How receptors talk to trimeric G proteins, *Curr. Opin. Cell Biol.* **9,** 134–142 (1997).
8. Rajagopal, S. Rajagopal, K. & Lefkowitz, R. J. Teaching old receptors new tricks: biasing seven-transmembrane receptors, *Nat. Rev. Drug Discov.* **9,** 373–386 (2010).
9. Whalen, E. J. Rajagopal, S. & Lefkowitz, R. J. Therapeutic potential of β-arrestin- and G protein-biased agonists, *Trends Mol. Med.* **17,** 126–139 (2011).
10. Azzi, M. *et al.* Beta-arrestin-mediated activation of MAPK by inverse agonists reveals distinct active conformations for G protein-coupled receptors, *Proc. Natl. Acad. Sci. U.S.A* **100,** 11406–11411 (2003).
11. Bosier, B. & Hermans, E. Versatility of GPCR recognition by drugs: from biological implications to therapeutic relevance, *Trends Pharmacol. Sci.* **28,** 438–446 (2007).
12. Kenakin, T. P. Cellular assays as portals to seven-transmembrane receptor-based drug discovery, *Nat. Rev. Drug Discov.* **8,** 617–626 (2009).
13. Smith, N. J. Bennett, K. A. & Milligan, G. When simple agonism is not enough: emerging modalities of GPCR ligands, *Mol. Cell. Endocrinol.* **331,** 241–247 (2011).
14. Urban, J. D. *et al.* Functional selectivity and classical concepts of quantitative pharmacology, *J. Pharmacol. Exp. Ther.* **320,** 1–13 (2007).
15. Kendall, R. T. *et al.* The {beta}-Arrestin Pathway-selective Type 1A Angiotensin Receptor (AT1A) Agonist [Sar1,Ile4,Ile8]Angiotensin II Regulates a Robust G Protein-independent Signaling Network, *J. Biol. Chem.* **286,** 19880–19891 (2011).
16. Antony, J. *et al.* Dualsteric GPCR targeting: a novel route to binding and signaling pathway selectivity, *FASEB J.* **23,** 442–450 (2009).
17. Mathiesen, J. M. *et al.* Identification of indole derivatives exclusively interfering with a G protein-independent signaling pathway of the prostaglandin D2 receptor CRTH2, *Mol. Pharmacol.* **68,** 393–402 (2005).
18. Galandrin, S. Oligny-Longpré, G. & Bouvier, M. The evasive nature of drug efficacy: implications for drug discovery, *Trends Pharmacol. Sci.* **28,** 423–430 (2007).

19. Dowal, L. *et al.* Identification of an antithrombotic allosteric modulator that acts through helix 8 of PAR1, *Proc. Natl. Acad. Sci. U.S.A* **108,** 2951–2956 (2011).

20. Baker, J. G. & Hill, S. J. Multiple GPCR conformations and signalling pathways: implications for antagonist affinity estimates, *Trends Pharmacol. Sci.* **28,** 374–381 (2007).

21. Maillet, E. L. *et al.* A novel, conformation-specific allosteric inhibitor of the tachykinin NK2 receptor (NK2R) with functionally selective properties, *FASEB J.* **21,** 2124–2134 (2007).

22. Hosoi, T. *et al.* Identification of a novel human eicosanoid receptor coupled to G(i/o), *J. Biol. Chem.* **277,** 31459–31465 (2002).

23. Jones, C. E. *et al.* Expression and characterization of a 5-oxo-6E,8Z,11Z,14Z-eicosatetraenoic acid receptor highly expressed on human eosinophils and neutrophils, *Mol. Pharmacol.* **63,** 471–477 (2003).

24. Grant, G. E. Rokach, J. & Powell, W. S. 5-Oxo-ETE and the OXE receptor, *Prostaglandins Other Lipid Mediat.* **89,** 98–104 (2009).

25. Irwin, J. J. & Shoichet, B. K. ZINC--a free database of commercially available compounds for virtual screening, *J. Chem. Inf. Model.* **45,** 177–182.

26. Trott, O. & Olson, A. J. AutoDock Vina: improving the speed and accuracy of docking with a new scoring function, efficient optimization, and multithreading, *J. Comput. Chem.* **31,** 455–461 (2010).

27. Papenfuhs, T. 2-Aminobenzothiazoles by oxidative cyclization of arylthioureas with sulfinyl chloride, *Angew. Chem. Int. Edit.* **21,** 541–542 (1982).

28. O'Flaherty, J. T. Taylor, J. S. & Kuroki, M. The coupling of 5-oxo-eicosanoid receptors to heterotrimeric G proteins, *J. Immunol.* **164,** 3345–3352 (2000).

29. Wu, D. Q. Huang, C. K. & Jiang, H. P. Roles of phospholipid signaling in chemoattractant-induced responses, *J. Cell Sci.* **113,** 2935–2940 (2000).

30. Jiang, H. *et al.* Pertussis toxin-sensitive activation of phospholipase C by the C5a and fMet-Leu-Phe receptors, *J. Biol. Chem.* **271,** 13430–13434 (1996).

31. Smrcka AV. G protein betagamma subunits: central mediators of G protein-coupled receptor signaling, *Cell Mol. Life. Sci.* **65,** 2191–2214 (2008).

32. Jiang, H. *et al.* Roles of phospholipase C beta2 in chemoattractant-elicited responses, *Proc. Natl. Acad. Sci. U.S.A* **94,** 7971–7975 (1997).

33. Li, Z. *et al.* Roles of PLC-beta2 and -beta3 and PI3Kgamma in chemoattractant-mediated signal transduction, *Science* **287,** 1046–1049 (2000).

34. Bonacci, T. M. *et al.* Differential targeting of Gbetagamma-subunit signaling with small molecules, *Science* **312,** 443–446 (2006).

35. Logothetis, D. E., Kurachi, Y., Galper, J., Neer, E. J. & Clapham, D. E. The beta gamma subunits of GTP-binding proteins activate the muscarinic K+ channel in heart, *Nature* **325,** 321–326 (1987).

36. Sadja, R., Alagem, N. & Reuveny, E. Gating of GIRK channels: details of an intricate, membrane-delimited signaling complex, *Neuron* **39,** 9–12 (2003).

37. Niswender, C. M. *et al.* A novel assay of Gi/o-linked G protein-coupled receptor coupling to potassium channels provides new insights into the pharmacology of the group III metabotropic glutamate receptors, *Mol. Pharmacol.* **73,** 1213–1224 (2008).

38. Galés, C. *et al.* Probing the activation-promoted structural rearrangements in preassembled receptor-G protein complexes, *Nat. Struct. Mol. Biol.* **13,** 778–786 (2006).

39. Rasmussen, S. G. F. *et al.* Crystal structure of the β(2) adrenergic receptor-Gs protein complex, *Nature* (2011).

40. Galés, C. *et al.* Real-time monitoring of receptor and G-protein interactions in living cells, *Nat. Methods* **2,** 177–184 (2005).

41. Bünemann, M. Frank, M. & Lohse, M. J. Gi protein activation in intact cells involves subunit rearrangement rather than dissociation, *Proc. Natl. Acad. Sci. U.S.A* **100,** 16077–16082 (2003).

42. Ashkenazi, A. *et al.* An M2 muscarinic receptor subtype coupled to both adenylyl cyclase and phosphoinositide turnover, *Science* **238,** 672–675 (1987).

43. Camps, M. *et al.* Isozyme-selective stimulation of phospholipase C-beta 2 by G protein beta gamma-subunits, *Nature* **360,** 684–686 (1992).

44. Katz, A. Wu, D. & Simon, M. I. Subunits beta gamma of heterotrimeric G protein activate beta 2 isoform of phospholipase C, *Nature* **360,** 686–689 (1992).

45. Cherfils, J. & Chabre, M. Activation of G-protein Galpha subunits by receptors through Galpha-Gbeta and Galpha-Ggamma interactions, *Trends Biochem. Sci.* **28,** 13–17 (2003).

46. Schröder, R. *et al.* Deconvolution of complex G protein-coupled receptor signaling in live cells using dynamic mass redistribution measurements, *Nat. Biotechnol.* **28,** 943–949 (2010).

47. Christiansen, E. *et al.* Discovery of potent and selective agonists for the free fatty acid receptor 1 (FFA(1)/GPR40), a potential target for the treatment of type II diabetes, *J. Med. Chem.* **51,** 7061–7064 (2008).

48. Schröder, R. *et al.* The C-terminal tail of CRTH2 is a key molecular determinant that constrains Galphai and downstream signaling cascade activation, *J. Biol. Chem.* **284,** 1324–1336 (2009).

49. Schmidt, J. *et al.* Selective orthosteric free fatty acid receptor 2 (FFA2) agonists: identification of the structural and chemical requirements for selective activation of FFA2 versus FFA3, *J. Biol. Chem.* **286,** 10628–10640 (2011).

50. Hartnell, A. *et al.* Identification of selective basophil chemoattractants in human nasal polyps as insulin-like growth factor-1 and insulin-like growth factor-2, *J. Immunol.* **173,** 6448–6457 (2004).

FIGURE LEGENDS

Figure 1: Structures, inhibitory efficacies and docking of OXE-R antagonists to the OXE-R.

(**a**) Chemical structures of Gü1157 and Gü1158. (**b**,**c**) Antagonistic properties of OXE-R antagonists in Ca^{2+} mobilization assays on HEK293 cells, transfected to co-express OXE-R and the promiscuous $G\alpha_{16}$ protein. 5-Oxo-ETE was used at 500 nM, a concentration corresponding to the EC_{80} of this ligand. 10 µM of Gü1157 and Gü1158, respectively, inhibit 5-oxo-ETE-mediated intracellular Ca^{2+} mobilization (**b**), but are inactive in Ca^{2+} assays when applied alone (**c**). In **b**, antagonists were pre-incubated with the cells at 37°C for 30 min before 5-oxo-ETE was added. Gü1157 inhibits shape change of human eosinophils stimulated with 5-oxo-ETE (**d**), but does not alter shape change of eosinophils triggered by activation of the prostaglandin D_2 receptor CRTH2 (**e**). (**f**) Computational model of the complex between Gü1157 and OXE-R. The color code of the helices is TM 2 (yellow), TM 3 (red), TM 5 (green), TM 6 (blue), TM 7 (brown).

Figure 2: Structure, docking and synthesis of the OXE-R antagonist Gü1654.

(**a**) Chemical structure of Gü1654. (**b**) Computational model of the complex between Gü1654 and OXE-R. The color code of the helices is as in **Figure 1**. (**c**) Synthetic scheme for Gü1654. a: MeI, K_2CO_3, H_2O, DMF; b: KSCN, AcCl, MeCN; c: KOH, EtOH; d: (1) $SOCl_2$, (2) H_2O, bolus alba; (3) aq. NH_3; e: $Ph_2CHCOCl$, 4-dimethylaminopyridine, *N*,*N*-diisopropylethylamine, THF.

Figure 3: Gü1654 is a functional antagonist of OXE-R in human recombinant and primary cells.

(**a**,**b**) Gü1654 antagonism of intracellular Ca^{2+} mobilization mediated by OXE-R. (**a**) OXE-dependent Ca^{2+} mobilization in the absence (vehicle) or presence of the indicated Gü1654 concentrations. Traces are from one representative out of three independent experiments. (**b**) Concentration-effect curves of 5-oxo-ETE in the absence (vehicle) and presence of Gü1654. Data are mean values + S.E. from at least three separate experiments. (**c**,**d**) Concentration-dependent inhibition by Gü1654 of neutrophil shape change (**c**) and neutrophil chemotaxis (**d**) triggered upon stimulation of cells with 5-oxo-ETE. (**e**,**f**) Concentration-dependent inhibition by Gü1654 of eosinophil shape change (**e**) and eosinophil chemotaxis (**f**) triggered upon stimulation of cells with 5-oxo-ETE. Data in **c** to **d** represent mean values + S.E. of three independent experiments.

Figure 4: **Gü1654 inhibits $G\alpha_{16}$ but not $G\alpha_i$-dependent signaling of OXE-R in recombinant and primary cells.**

(**a**) Inhibition of forskolin-stimulated cAMP production by 5-oxo-ETE in the absence (vehicle) and presence of Gü1654 in human neutrophils. Gü1654 does not interfere with the ability of 5-oxo-ETE to lower intracellular cAMP production. (**b**) Inhibition of forskolin-stimulated cAMP production by 5-oxo-ETE in the absence (vehicle) and presence of the indicated Gü1654 concentrations in HEK293 cells stably transfected to co-express OXE-R and $G\alpha_{16}$. PTX pre-treatment (50 ng/ml) for 18-24 h prior to the cAMP inhibition assay abolishes the functional 5-oxo-ETE response and confirms its $G\alpha_i$ origin. Gü1654 fails to inhibit OXE-R signaling through $G\alpha_i$ in the HEK293 cellular background. (**c**) Lack of inhibitory efficacy of Gü1654 on the OXE-R-$G\alpha_i$ signaling pathway as determined in label-free holistic dynamic mass redistribution (DMR)

assays. HEK293 cells transiently transfected to express OXE-R were challenged with 5-oxo-ETE in the absence (vehicle) or presence of Gü1654. $G\alpha_i$ origin of the functional response was verified by abrogation of the agonist DMR signal with PTX (50 ng/ml). (**d**,**e**) Gü1654 attenuates OXE-R-$G\alpha_{16}$ signaling in a concentration-dependent manner. HEK293 cells stably expressing OXE-R and $G\alpha_{16}$ were pre-treated with PTX (50 ng/ml, 18 h) to silence $G\alpha_i$ activity and DMR was monitored in real time as a measure of OXE-R-$G\alpha_{16}$ engagement after stimulation with 3 µM 5-oxo-ETE. Depicted in **d** are original optical traces that are representative of at least three independent experiments, data in **e** represent mean values + S.E of three such experiments.

Figure 5: Gü1654 is an efficacious antagonist of 5-oxo-ETE-dependent Ca^{2+} flux in human neutrophils and eosinophils.

(**a**,**b**) 5-Oxo-ETE mobilizes Ca^{2+} from intracellular stores in human neutrophils (**a**) and eosinophils (**b**), respectively. Both effects are sensitive to pre-treatment with pertussis toxin (3 µg/ml; 1 h). (**c**,**d**) $G\alpha_i$-sensitive, 5-oxo-ETE-mediated Ca^{2+} release in human neutrophils (**c**) and eosinophils (**d**) is completely blunted by pre-treatment with Gü1654. (**e**,**f**) 5-Oxo-ETE-mediated Ca^{2+} release in human neutrophils (**e**) and eosinophils (**f**) is sensitive to pre-treatment with the phospholipase Cβ inhibitor U73122 but not its inactive analog U73343. Data in **a** to **f** represent mean values + S.E of three separate experiments.

Figure 6: Gü1654 is a specific inhibitor of OXE-R-βγ signaling but does not interfere non-specifically with signaling at or downstream of Gβγ.

(**a**) 5-Oxo-ETE increases inositol phosphate (IP) production in HEK293 cells transfected to express OXE-R, $G\beta_1$, and $G\gamma_2$ in a Gβγ-dependent manner. 5-Oxo-ETE-mediated IP production is completely blunted by pre-treatment with Gü1654 or the small molecule Gβγ inhibitor gallein[34]. In contrast, inositolphosphate production triggered upon stimulation with carbachol, that acts via endogenous $G\alpha_q$-linked muscarinic receptors, is unaffected by both gallein and Gü1654. Antagonists (gallein and Gü1654) were pre-incubated for 30 min at 37°C before IP production was stimulated with 5-oxo-ETE. Data in **a** are mean values + S.E. of three to eight independent experiments each performed in quadruplicate. ***, significant effect to basal IP1 levels; ###, significant effect to 5-oxo-ETE; §§§, significant effect to carbachol; ns, non-significant effect to carbachol. ***, ### and §§§, $p < 0.001$ according to one-way ANOVA with Bonferroni's multiple comparison test. (**b**) HEK-GIRK cells co-expressing the OXE-R were loaded with the thallium indicator dye BTC-AM and thallium conductance was recorded over time after stimulation with the indicated concentrations of 5-oxo-ETE as described in detail in **Supplementary Online methods**. All traces were vehicle-corrected (representative experiment, n= 3). (**c**) Concentration-effect curve for 5-oxo-ETE calculated from the slopes of the individual traces in the time window of 10 - 20 seconds and normalized to a maximally effective concentration of 5-oxo-ETE. Pre-treatment of cells with 80 ng/ml of PTX over night abolishes 5-oxo-ETE-mediated thallium flux. Shown are mean values ± S.E (n= 3). (**d**) Pre-treatment of HEK-GIRK cells co-expressing the OXE-R with the indicated concentrations of Gü1654 completely dampens thallium flux induced by 2 nM 5-oxo-ETE-mediated. Data shown are mean values + S.E (n= 3).

Figure 7: Gü1654 selectively targets Gβγ-but not Gαi-signaling within Gαi-βγ heterotrimers in a receptor-specific manner.

Bioluminescence resonance energy transfer (BRET) assay between OXE-R fused to Renilla Luciferase (RLuc) and GFP10-Gγ2 (**a**) or GFP10-Gβ1 (**b**) in HEK293 cells expressing the labeled constructs along with unlabeled Gαi2, Gβ1, or Gγ2. 5-Oxo-ETE stimulation leads to robust elevation in BRET between OXE-R-RLuc and the Gβγ probes (**a**,**b**). Gü1654 diminishes OXE-R-Gγ BRET by over 40% (**a**) but does hardly affect OXE-R-Gβ BRET (**b**). (**c**,**d**) Gü1654 does not significantly reduce basal BRET between OXE-R-RLuc and GFP10-Gγ2 or GFP10-Gβ1. (**e**) Gü1654 does not inhibit BRET between the nicotinic acid receptor HM74A fused to RLuc (HM74A-RLuc) and GFP10-Gγ2 upon stimulation with the HM74A agonist nicotinic acid (NA) in HEK293 cells transiently expressing the labeled BRET partners. (**f**) Gü1654 fails to prevent BRET alterations induced with 5-oxo-ETE in HEK293 cells transiently transfected to express OXE-R, Gαi1-91RLuc and GFP10-Gγ2. This BRET assay setup analyzes the consequences of receptor activation on Gα-βγ interaction. 5-oxo-ETE promotes a robust BRET reduction, reflecting structural rearrangement of Gα and Gβγ that is indicative of an opening of the nucleotide binding pocket of the heterotrimer[37]. Data in **a** to **f** are mean values + S.E. of two to seven independent experiments, each performed in triplicate. **a**,*, $p < 0.05$; ***, $p < 0.001$, compared to 5-oxo-ETE-mediated BRET; **b**, **f**, ns, compared to 5-oxo-ETE-mediated BRET;**c**, **d**, ns, compared to BRET in the absence of 5-oxo-ETE;**e**, ns, compared to nicotinic acid (NA) mediated BRET according to one-way ANOVA with Bonferroni's multiple comparison test.

Figure 8: Schematic model of Gβγ-biased antagonism.

(**a**) G protein-coupled receptor and heterotrimeric Gαβγ protein in the resting state. The receptor is not occupied by an agonist and the heterotrimer contains GDP bound to its Gα subunit. (**b**) Occupation of the receptor by an activating ligand (yellow triangle) induces a conformational change of the receptor protein or stabilizes an active receptor conformation and initiates the GDP-GTP off-on cycle. Guanine nucleotide exchange is accompanied by intramolecular rearrangement of Gα relative to Gβγ, each of which may activate their downstream effectors.. (**c**) Co-occupation of receptor with an agonist and a Gβγ-biased antagonist (black rectangle). In the presence of the biased antagonist, the receptor spares signaling via the Gβγ route but retains the ability to promote GDP-GTP exchange and activate Gα downstream targets. (**d**) For comparison, occupation of the receptor with a classical competitive (unbiased) antagonist (purple diamond) is shown. The entire set of receptor activation signals is disabled.

Figure 1

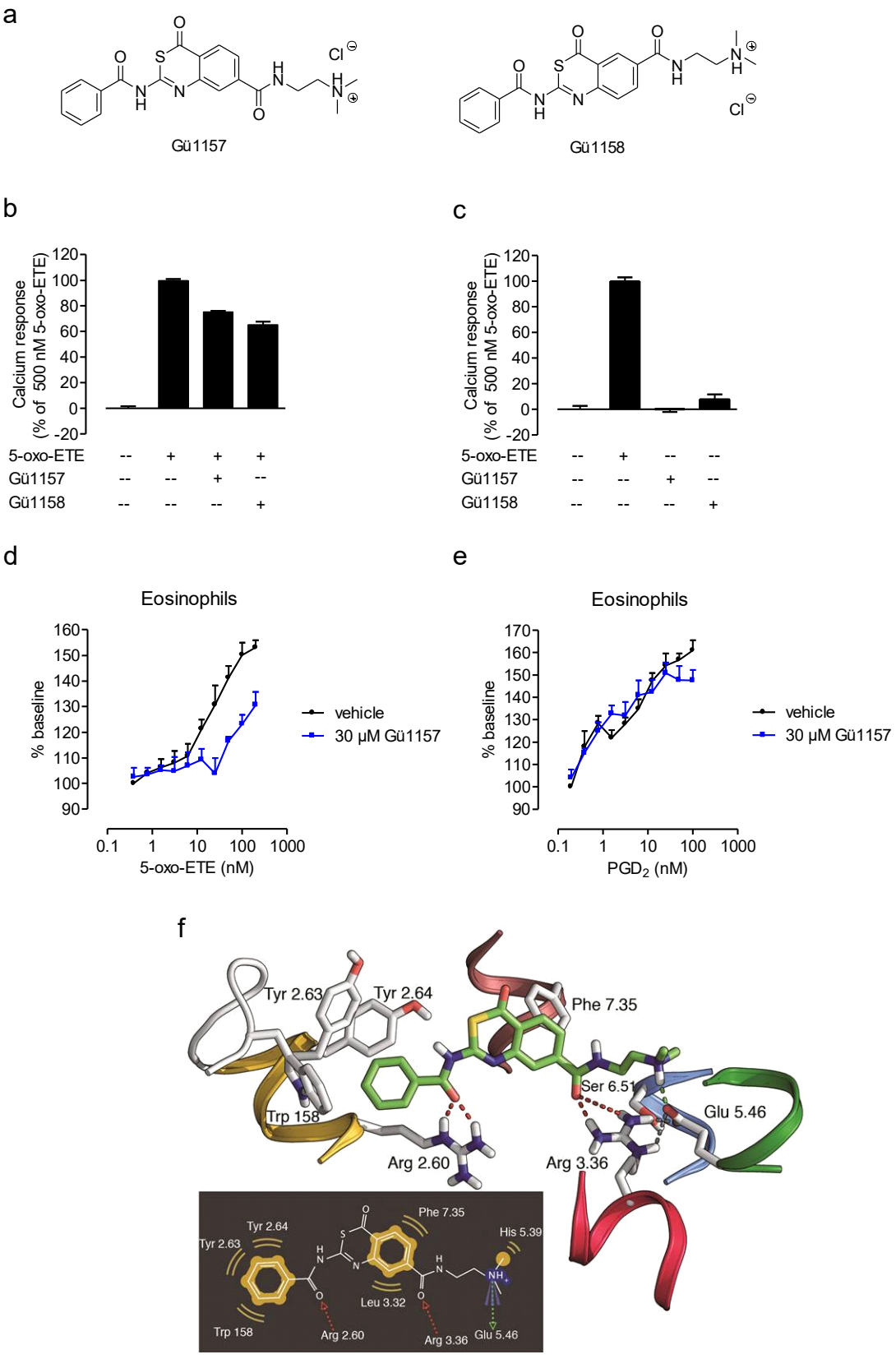
a
Gü1157
Gü1158
b
Calcium response (% of 500 nM 5-oxo-ETE)
5-oxo-ETE
Gü1157
Gü1158
c
Calcium response (% of 500 nM 5-oxo-ETE)
5-oxo-ETE
Gü1157
Gü1158
d
Eosinophils
% baseline
5-oxo-ETE (nM)
vehicle
30 μM Gü1157
e
Eosinophils
% baseline
PGD2 (nM)
vehicle
30 μM Gü1157
f
Tyr 2.63
Tyr 2.64
Phe 7.35
Ser 6.51
Glu 5.46
Trp 158
Arg 2.60
Arg 3.36
His 5.39
Leu 3.32

Figure 2

a

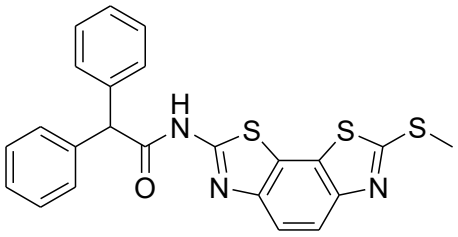

Gü1654

b

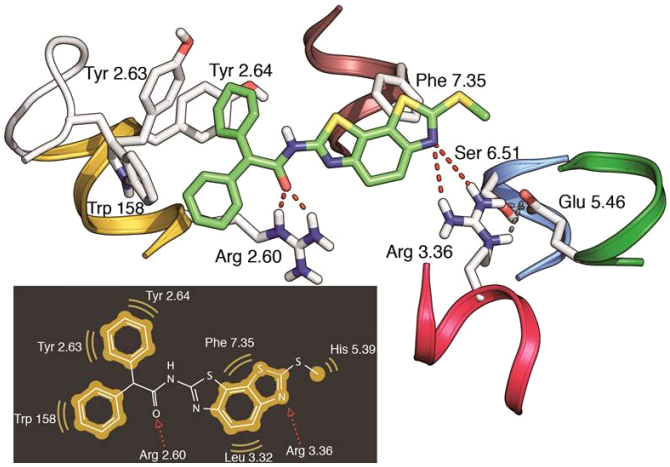

c

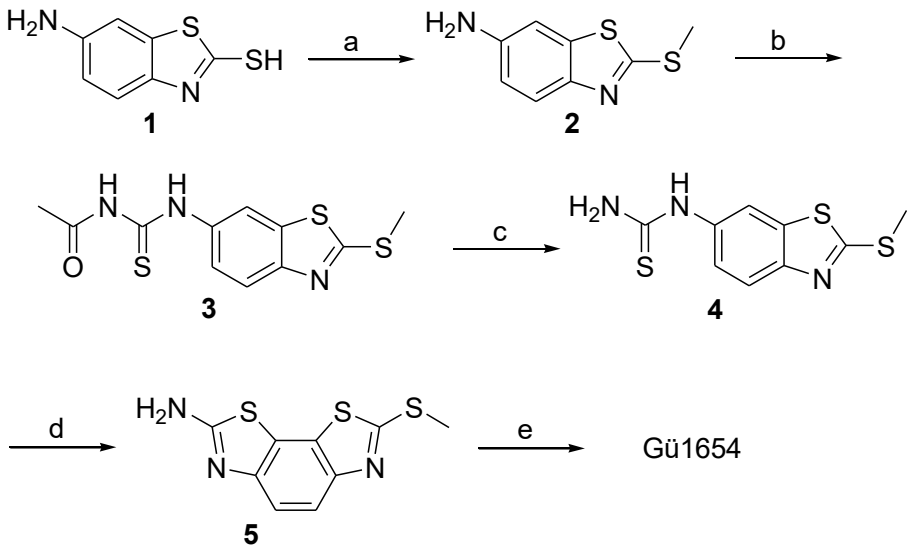

Figure 3

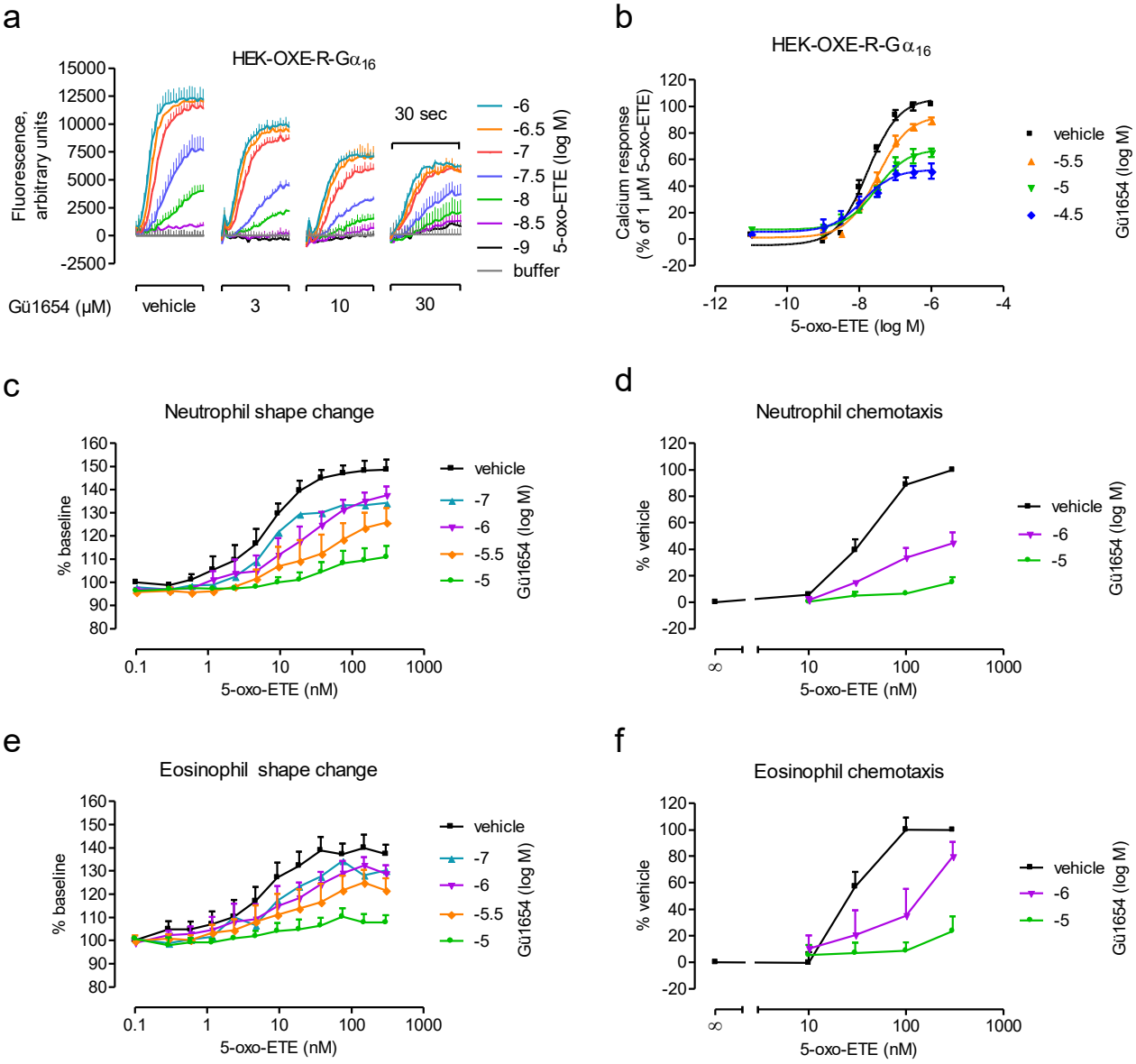
a
HEK-OXE-R-Gα16
Fluorescence, arbitrary units
15000
12500
10000
7500
5000
2500
0
-2500
30 sec
-6
-6.5
-7
-7.5
-8
-8.5
-9
buffer
5-oxo-ETE (log M)
Gü1654 (μM)
vehicle
3
10
30
b
HEK-OXE-R-Gα16
Calcium response (% of 1 μM 5-oxo-ETE)
120
100
80
60
40
20
0
-20
-12
-10
-8
-6
-4
5-oxo-ETE (log M)
vehicle
-5.5
-5
-4.5
Gü1654 (log M)
c
Neutrophil shape change
% baseline
160
150
140
130
120
110
100
90
80
0.1
1
10
100
1000
5-oxo-ETE (nM)
vehicle
-7
-6
-5.5
-5
Gü1654 (log M)
d
Neutrophil chemotaxis
% vehicle
120
100
80
60
40
20
0
-20
∞
10
100
1000
5-oxo-ETE (nM)
vehicle
-6
-5
Gü1654 (log M)
e
Eosinophil shape change
% baseline
160
150
140
130
120
110
100
90
80
0.1
1
10
100
1000
5-oxo-ETE (nM)
vehicle
-7
-6
-5.5
-5
Gü1654 (log M)
f
Eosinophil chemotaxis
% vehicle
120
100
80
60
40
20
0
-20
∞
10
100
1000
5-oxo-ETE (nM)
vehicle
-6
-5
Gü1654 (log M)

Figure 4

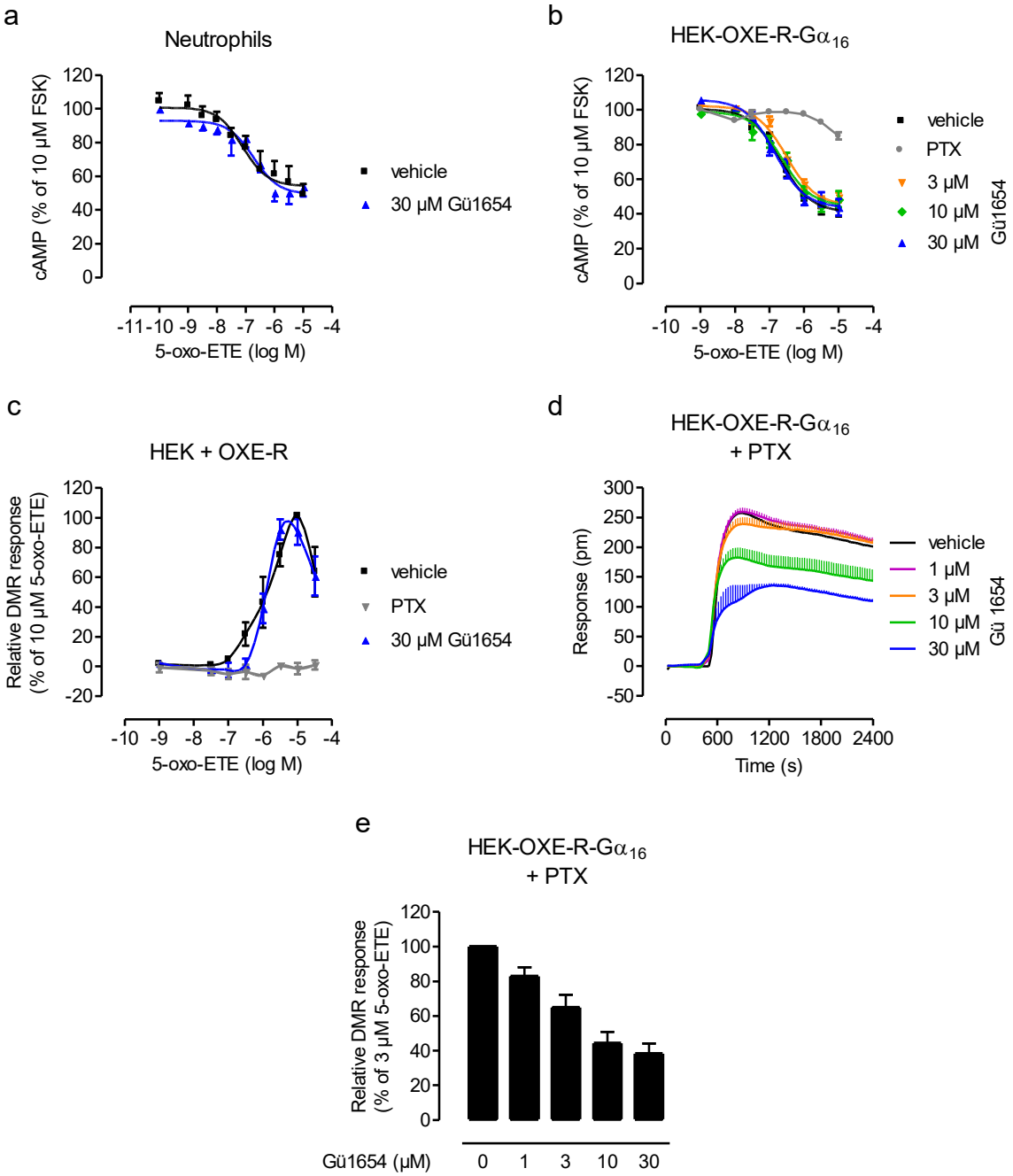
a
Neutrophils
cAMP (% of 10 µM FSK)
120
100
80
60
40
20
0
-11 -10 -9 -8 -7 -6 -5 -4
5-oxo-ETE (log M)
vehicle
30 µM Gü1654
b
HEK-OXE-R-Gα16
cAMP (% of 10 µM FSK)
120
100
80
60
40
20
0
-10 -9 -8 -7 -6 -5 -4
5-oxo-ETE (log M)
vehicle
PTX
3 µM
10 µM
30 µM
Gü1654
c
HEK + OXE-R
Relative DMR response
(% of 10 µM 5-oxo-ETE)
120
100
80
60
40
20
0
-20
-10 -9 -8 -7 -6 -5 -4
5-oxo-ETE (log M)
vehicle
PTX
30 µM Gü1654
d
HEK-OXE-R-Gα16
+ PTX
Response (pm)
300
250
200
150
100
50
0
-50
0 600 1200 1800 2400
Time (s)
vehicle
1 µM
3 µM
10 µM
30 µM
Gü 1654
e
HEK-OXE-R-Gα16
+ PTX
Relative DMR response
(% of 3 µM 5-oxo-ETE)
120
100
80
60
40
20
0
Gü1654 (µM)
0 1 3 10 30

Figure 5

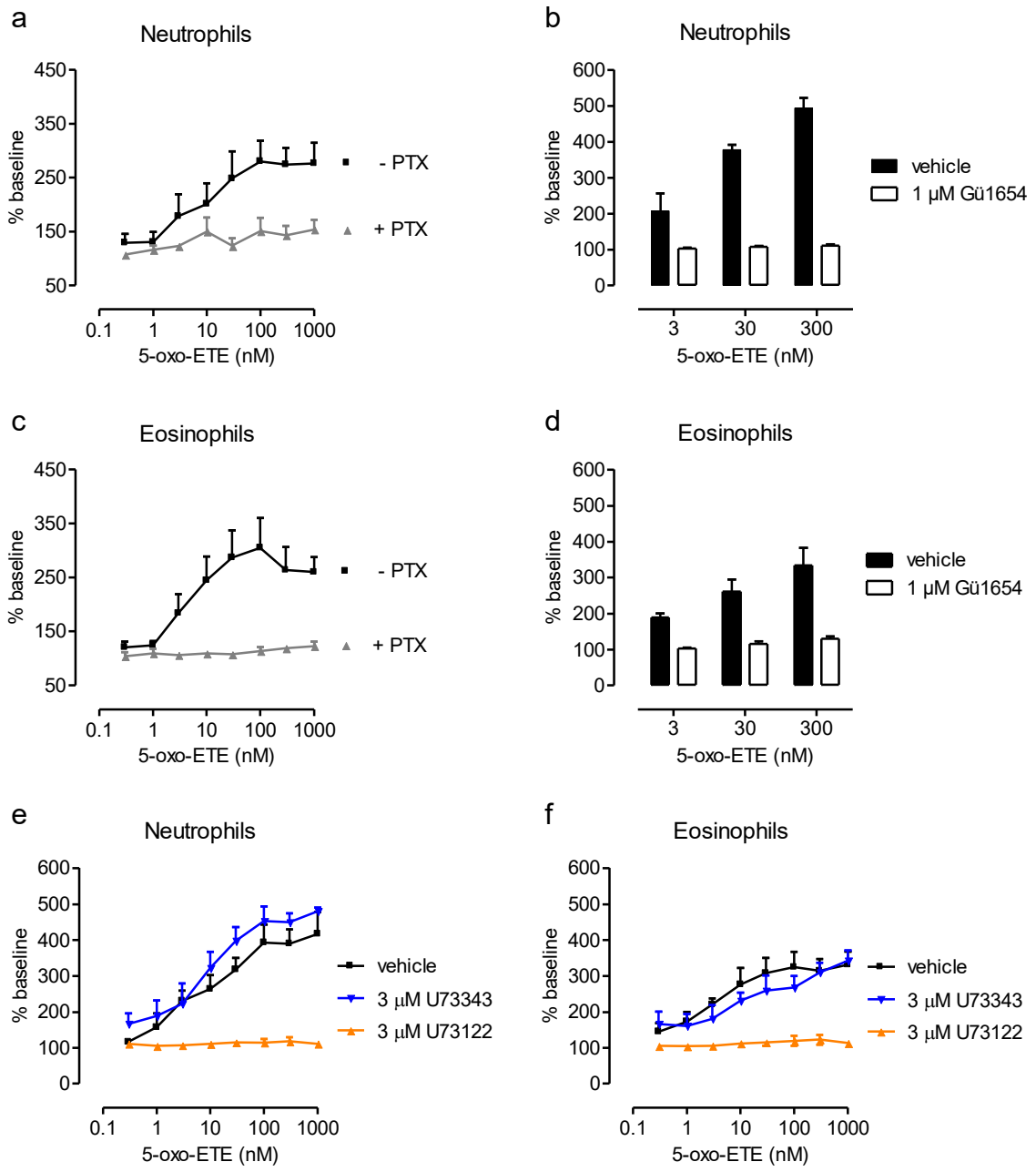
a
Neutrophils
% baseline
450
350
250
150
50
0.1
1
10
100
1000
5-oxo-ETE (nM)
- PTX
+ PTX
b
Neutrophils
% baseline
600
500
400
300
200
100
0
3
30
300
5-oxo-ETE (nM)
vehicle
1 μM Gü1654
c
Eosinophils
% baseline
450
350
250
150
50
0.1
1
10
100
1000
5-oxo-ETE (nM)
- PTX
+ PTX
d
Eosinophils
% baseline
600
500
400
300
200
100
0
3
30
300
5-oxo-ETE (nM)
vehicle
1 μM Gü1654
e
Neutrophils
% baseline
600
500
400
300
200
100
0
0.1
1
10
100
1000
5-oxo-ETE (nM)
vehicle
3 μM U73343
3 μM U73122
f
Eosinophils
% baseline
600
500
400
300
200
100
0
0.1
1
10
100
1000
5-oxo-ETE (nM)
vehicle
3 μM U73343
3 μM U73122

Figure 6

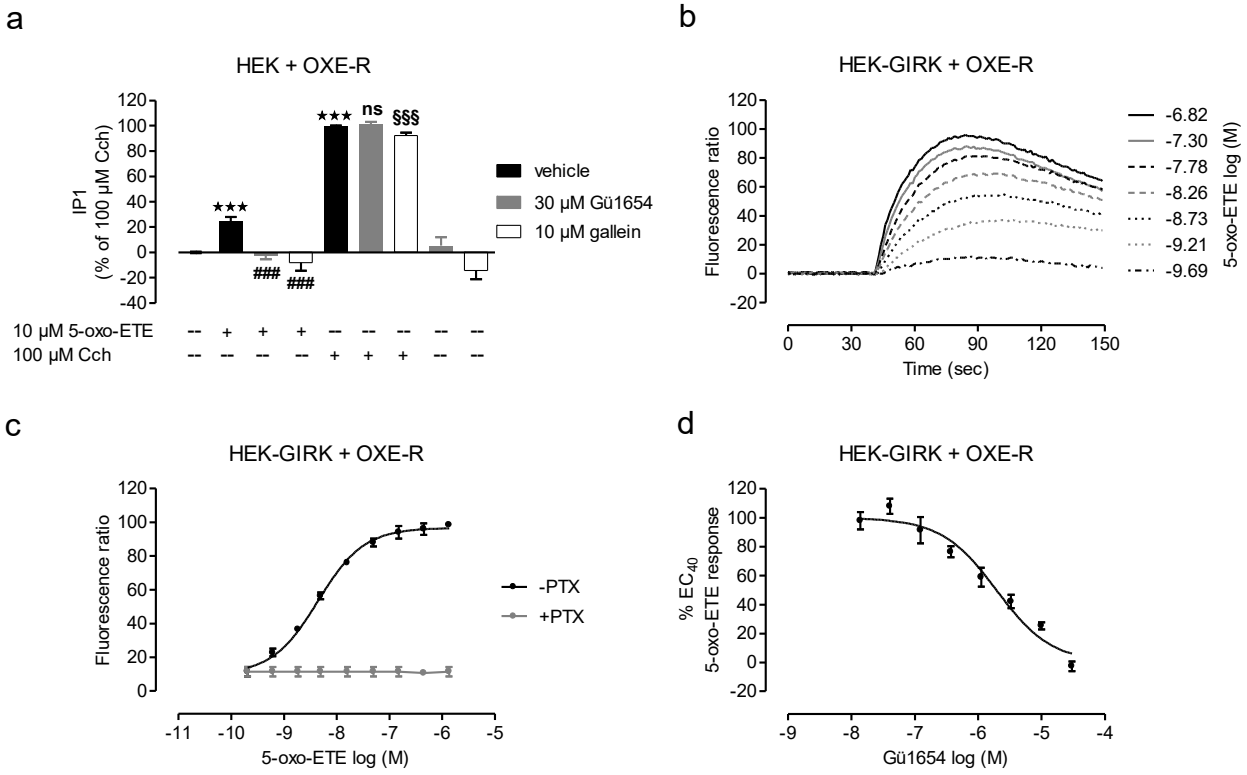
a
HEK + OXE-R
IP1
(% of 100 µM Cch)
120
100
80
60
40
20
0
-20
-40
★★★
★★★
###
###
ns
§§§
vehicle
30 µM Gü1654
10 µM gallein
10 µM 5-oxo-ETE -- + + + -- -- -- -- --
100 µM Cch -- -- -- -- + + + -- --
b
HEK-GIRK + OXE-R
Fluorescence ratio
120
100
80
60
40
20
0
-20
0
30
60
90
120
150
Time (sec)
-6.82
-7.30
-7.78
-8.26
-8.73
-9.21
-9.69
5-oxo-ETE log (M)
c
HEK-GIRK + OXE-R
Fluorescence ratio
120
100
80
60
40
20
0
-11
-10
-9
-8
-7
-6
-5
5-oxo-ETE log (M)
-PTX
+PTX
d
HEK-GIRK + OXE-R
% EC40
5-oxo-ETE response
120
100
80
60
40
20
0
-20
-9
-8
-7
-6
-5
-4
Gü1654 log (M)

Figure 7

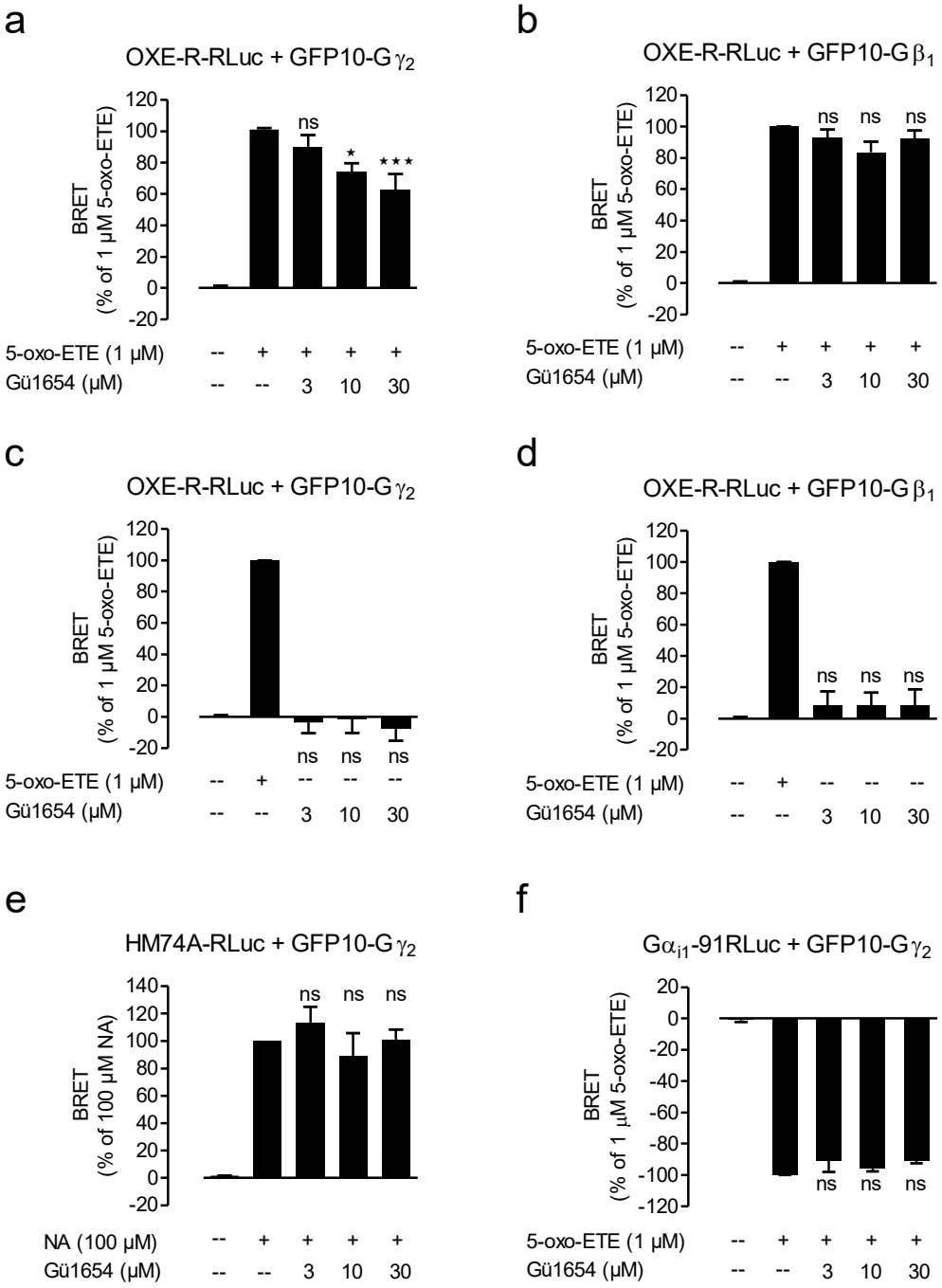
a
OXE-R-RLuc + GFP10-Gγ2
BRET (% of 1 µM 5-oxo-ETE)
ns
*
***
5-oxo-ETE (1 µM) -- + + + +
Gü1654 (µM) -- -- 3 10 30
b
OXE-R-RLuc + GFP10-Gβ1
BRET (% of 1 µM 5-oxo-ETE)
ns ns ns
5-oxo-ETE (1 µM) -- + + + +
Gü1654 (µM) -- -- 3 10 30
c
OXE-R-RLuc + GFP10-Gγ2
BRET (% of 1 µM 5-oxo-ETE)
ns ns ns
5-oxo-ETE (1 µM) -- + -- -- --
Gü1654 (µM) -- -- 3 10 30
d
OXE-R-RLuc + GFP10-Gβ1
BRET (% of 1 µM 5-oxo-ETE)
ns ns ns
5-oxo-ETE (1 µM) -- + -- -- --
Gü1654 (µM) -- -- 3 10 30
e
HM74A-RLuc + GFP10-Gγ2
BRET (% of 100 µM NA)
ns ns ns
NA (100 µM) -- + + + +
Gü1654 (µM) -- -- 3 10 30
f
Gαi1-91RLuc + GFP10-Gγ2
BRET (% of 1 µM 5-oxo-ETE)
ns ns ns
5-oxo-ETE (1 µM) -- + + + +
Gü1654 (µM) -- -- 3 10 30

Figure 8

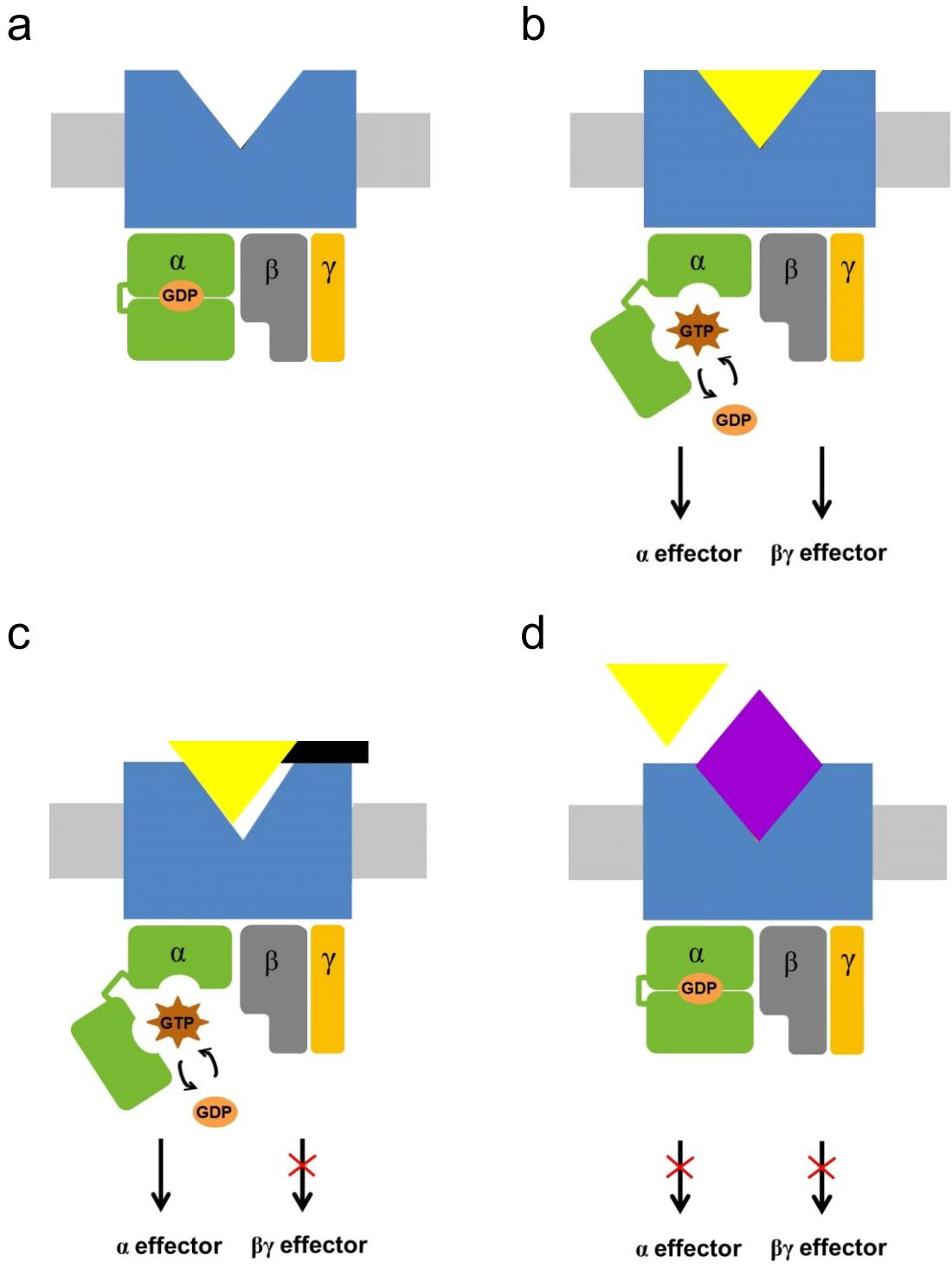
a
α
GDP
β
γ
b
α
GTP
GDP
β
γ
α effector
βγ effector
c
α
GTP
GDP
β
γ
α effector
βγ effector
d
α
GDP
β
γ
α effector
βγ effector